

Simulation of current-filament dynamics and relaxation in the Pegasus ST

J.B. O'Bryan and C.R. Sovinec

University of Wisconsin–Madison

55th Annual APS-DPP Meeting
November 12, 2013



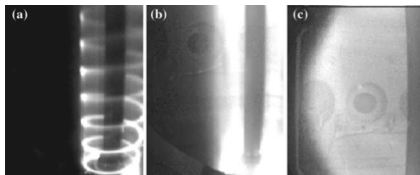
Fluid-based computation predicts that current filament merger and reconnection is an important process for non-inductive startup with localized helicity injection.

- Introduction
- Computational Model
- Current Filament Merger and Reconnection
- Poloidal Flux Development
- Plasma Symmetrization
- Summary and Conclusions

Localized helicity injection (LHI) is being investigated as a means of non-solenoidal startup on the Pegasus ST.

- A collaboration between Pegasus and NSTX-U is charged with developing and implementing a 1 MA LHI startup system on NSTX-U. (NSTX-U Research Plan 2014-2018. §11.2.27.)
- While the initial helical and final symmetric plasma states are well diagnosed in the experiment, the dynamics of the relaxation process have yet to be directly observed.
 - Diagnostics that provide multidimensional information (e.g. visible light) are unable to temporally resolve the helical filament interactions.
 - Visible light images, in particular, may not be representative of the magnetic field structure throughout the relaxation process.
 - Magnetic diagnostics resolve fluctuations temporally, but are incapable of spatially resolving fine-scale structure.

Visible light images of discharges formed using two injectors mounted in the lower divertor. (Eidietis, et. al. *J. Fus. En.* 2007.)



Our computations solve the low-frequency two-fluid model starting from vacuum magnetic field and 'cold fluid.'

$$\frac{\partial n}{\partial t} + \nabla \cdot (n\mathbf{v}) = 0$$

$$\rho \left(\frac{\partial \mathbf{v}}{\partial t} + \mathbf{v} \cdot \nabla \mathbf{v} \right) = \mathbf{J} \times \mathbf{B} - \nabla p + \nabla \cdot (nm\nu \underline{\mathbf{W}}) \quad \text{where } \underline{\mathbf{W}} = \nabla \mathbf{v} + \nabla \mathbf{v}^T - (2/3)(\nabla \cdot \mathbf{v})\mathbf{I}$$

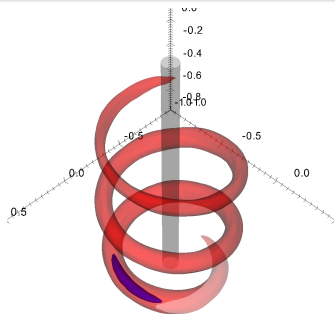
$$\frac{2n}{3} \left(\frac{\partial T_e}{\partial t} + \mathbf{v} \cdot \nabla T_e \right) = -nT_e \nabla \cdot \mathbf{v} - \nabla \cdot [\kappa_{\parallel e} \hat{\mathbf{b}}\hat{\mathbf{b}} + \kappa_{\perp e} \mathbf{I}] \cdot \nabla T_e + n\sigma (T_i - T_e) + \eta J^2$$

$$\frac{2n}{3} \left(\frac{\partial T_i}{\partial t} + \mathbf{v} \cdot \nabla T_i \right) = -nT_i \nabla \cdot \mathbf{v} - \nabla \cdot [\kappa_{\parallel i} \hat{\mathbf{b}}\hat{\mathbf{b}} + \kappa_{\perp i} \mathbf{I}] \cdot \nabla T_i + n\sigma (T_e - T_i) + \underbrace{Q_i}_{\text{heat source}}$$

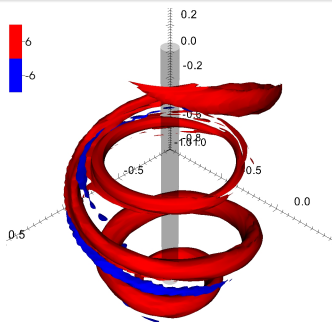
$$\frac{\partial \mathbf{B}}{\partial t} + \nabla \times \left[\eta \mathbf{J} - \underbrace{\frac{\eta \lambda_{inj} \mathbf{B}}{\mu_0}}_{\text{current source}} - \mathbf{v} \times \mathbf{B} + \frac{\mathbf{J} \times \mathbf{B}}{n_e e} - \frac{\nabla p_e}{n_e e} \right] = 0 \quad \text{where } \mathbf{J} = \mu_0^{-1} \nabla \times \mathbf{B}$$

- The computations model the whole evolution of the current filaments using realistic, evolving, locally computed transport coefficients.
- Only the helicity injector **current** and **heat** sources are prescribed: all dynamics follow self-consistently from the model above.
- Neutrals, ionization, and recombination are not modeled.
- The NIMROD code (nimrodteam.org) is used to solve these systems.

Like the experiment, the only source of current drive during the formation phase is the helicity injector.



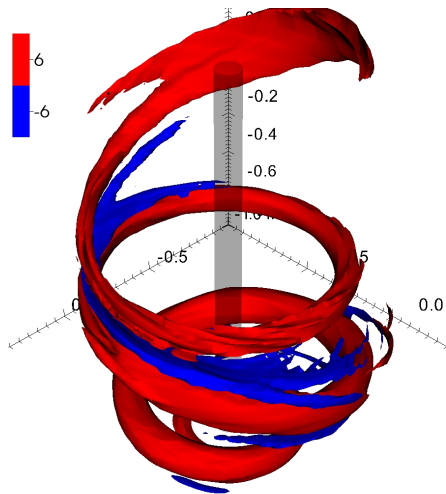
source half-max (blue) and $\mu_0 J_{\parallel}/B = 1 \text{ m}^{-1}$ (red) at $I_p \approx 1 \text{ kA}$.



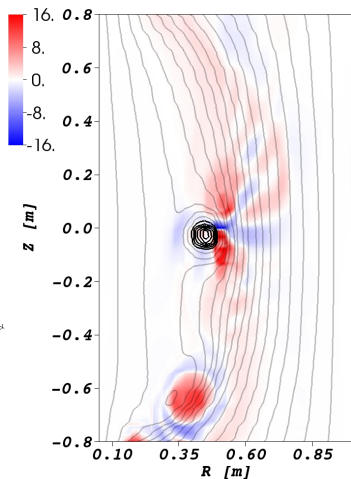
$\mu_0 J_{\parallel}/B = \pm 6 \text{ m}^{-1}$ at $I_p \approx 6.5 \text{ kA}$

- Initially, current streams along the vacuum magnetic field lines establishing a helical current channel.
- After localized reversal of the poloidal magnetic field, the attractive Lorentz force between adjacent passes is sufficient to drive magnetic reconnection (indicated by the presence of a reversed current sheet).
- A transit of the current channel tilts into the horizontal plane and is released, converting helical flux from the source into poloidal flux.

Computation shows concentration of poloidal flux where a current ring forms.

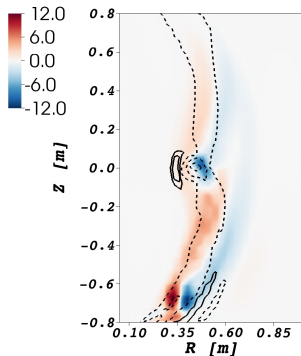


$\mu_0 J_{\parallel} / B$ [m^{-1}]

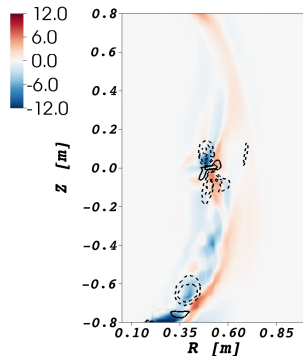


$\mu_0 J_{\parallel} / B$ [m^{-1}] with
logarithmic poloidal flux contours

The tilting of a transit of the filament into the horizontal plane constitutes dynamo-like activity that affects the global distribution.



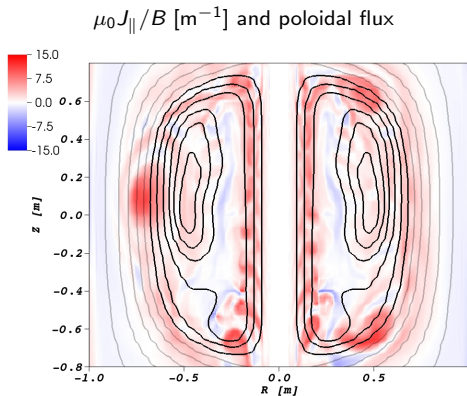
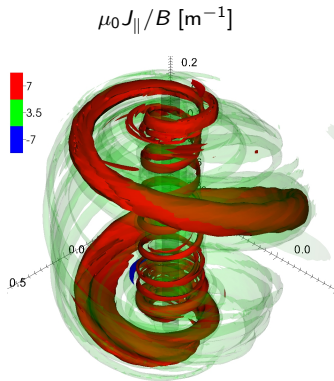
Contours of $-2\pi R \langle \tilde{\mathbf{v}} \times \tilde{\mathbf{B}} \rangle_{\phi}$ [V],
 $\langle \mu_0 J_{\parallel} / B \rangle < 0$ (solid), $\langle \mu_0 J_{\parallel} / B \rangle > 0$ (dotted)



Contours $2\pi R \langle \tilde{\mathbf{J}} \times \tilde{\mathbf{B}} \rangle_{\phi} / ne$ [V],
 $\mu_0 J_{\parallel} / B < 0$ (solid), $\mu_0 J_{\parallel} / B > 0$ (dotted)

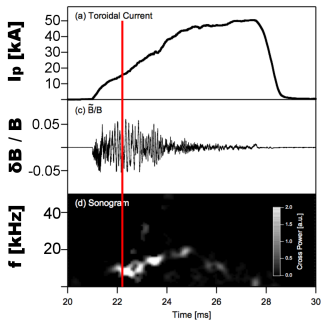
- Correlations of toroidally asymmetric fluctuations lead to mean electric fields that increase that increase the energy density in the mean field when $\langle \mathbf{E} \rangle \cdot \langle \mathbf{J} \rangle < 0$.
- The MHD dynamo effect (left) transfers the bulk of the energy to the ring.
- The Hall dynamo effect (right) acts on a scale smaller than the ring.

After a poloidal field null forms near the central column, a hollow current shell forms around a region of amplified flux.

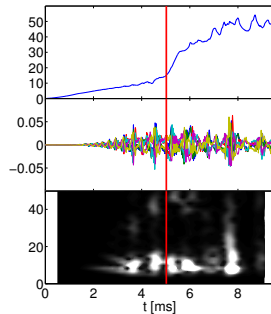


- The current on the inboard side is initially diffuse, but coalesces into a coherent channel (left) as I_p increases.
- A large region of significant poloidal flux amplification (right) has developed over many relaxation events.
- Even late in time, the plasma retains its filamentary structure during active helicity injection.

A synthetic Mirnov array at the outboard midplane records magnetic fluctuation amplitudes ($\delta B/B_0 \sim 5\%$) and cross power spectra consistent with experimental observations.



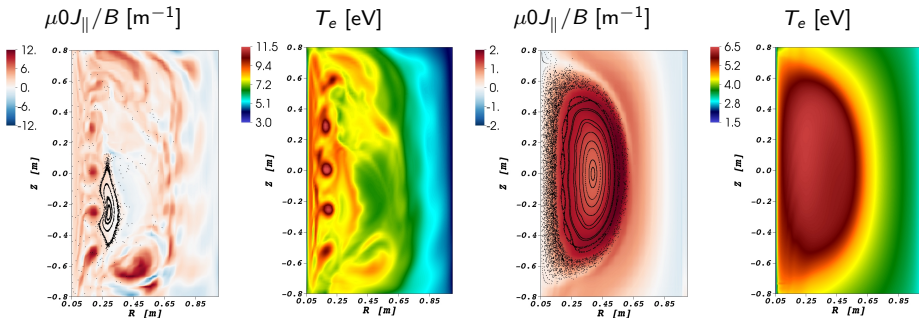
Pegasus Experimental Data



Computational Results

- The computations have a more gradual rate of helicity injection than the experiment, so comparisons focus on **after** global poloidal field null formation (indicated by the red lines).
- The MHD activity (~ 10 kHz) corresponds to the reconnection event and abrupt change in current channel winding.

As LHI plasmas are intended to transition to other forms of current drive, the ability to relax into a configuration with closed flux surfaces is critical.



LHI driven phase

decay phase

- Closed flux surfaces form rapidly and encompass a large plasma volume after cessation of current drive.
- The current profile of the relaxing plasma remains hollow, but the pressure profile relaxes to a centrally peaked configuration.

Summary and Conclusions

- The release of current rings from helical filaments provides a new phenomenological understanding for filament relaxation in Pegasus.
1 2
- The current filament dynamics, predicted to be important for LHI startup, are not readily apparent from visible light spectroscopy.
- The MHD activity observed with the synthetic Mirnov diagnostic is consistent with experimental Mirnov observations.
- Measurements from new magnetic sensor currently under construction will assist in validating this model.
- The current rings provide the mechanism for poloidal flux amplification over multiple reconnection events, resulting in a **plasma suitable for transition to other forms of current drive.**

¹J.B. O'Bryan, C.R. Sovinec, and T.M. Bird. *Phys. Plas.* 2012.

²J.B. O'Bryan and C.R. Sovinec. UW-CPTC Report 13-6. Submitted to *PPCF*. 2013.